Terr. Atmos. Ocean. Sci., Vol. 19, No. 4, 363-376, August 2008 doi: 10.3319/TAO.2008.19.4.363(IMAGES)

Sea Surface Temperature, Productivity, and Terrestrial Flux Variations of the Southeastern South China Sea over the Past 800000 Years (IMAGES MD972142)

Liang-Jian Shiau[1], Pai-Sen Yu[1], Kuo-Yen Wei[2], Masanobu Yamamoto[3], Teh-Quei Lee[4], Ein-Fen Yu[5], Tien-Hsi Fang[6], and Min-Te Chen[1, *]

[1] *Institute of Applied Geosciences, National Taiwan Ocean University, Keelung, Taiwan, ROC*
[2] *Department of Geosciences, National Taiwan University, Taipei, Taiwan, ROC*
[3] *Graduate School of Environmental Earth Science, Hokkaido University, Sapporo, Japan*
[4] *Institute of Earth Sciences, Academia Sinica, Taipei, Taiwan, ROC*
[5] *Department of Earth Sciences, National Taiwan Normal University, Taipei, Taiwan, ROC*
[6] *Department of Marine Environmental Informatics, National Taiwan Ocean University, Keelung, Taiwan, ROC*

Received 8 June 2006, accepted 21 September 2007

ABSTRACT

Variations in sea surface temperature (SST), productivity, and biogenic components such as total organic carbon (TOC), carbonate, and opal contents measured from IMAGES (International Marine Global Changes Study) core MD972142 provide information about long-term paleoceanographic changes during the past ~870000 years in the southeastern South China Sea (SCS). MD972142 $U^{k'}_{37}$-SSTs varied from 25 to 29°C, paralleling the glacial to interglacial changes. MD972142 biogenic components show relatively high carbonate and opal, and low TOC contents in interglacial stages, and low carbonate and opal and high TOC contents in glacial stages, and these variations appear to be sensitive to regional terrestrial sediment input and productivity. Our analysis indicates that the MD972142 carbonate record is primarily controlled by terrestrial sediment inputs that are associated with sea level fluctuations during past glacial-interglacial stages. The TOC record reflects past glacial-interglacial changes in both monsoon-induced productivity and terrestrial organic matter input in the SCS. The TOC record exhibits several short-term peaks that are associated with lower $U^{k'}_{37}$-SSTs (especially in MIS 2 - 4, 10, 12), perhaps implying a much strengthened winter monsoon. The opal record shows relatively high content in most interglacial stages, which appears to be linked to increased summer monsoon upwelling or increased siliceous sediment input by more precipitation and river runoff during warm climate conditions. The TOC and opal contents both show long-term increasing trends since the mid-Brunhes, most noticeably from ~330 kya. The long-term trends observed in this study are most likely attributable to changes in SCS hydrography, productivity, and/or preservation in response to the increased strength of the East Asian monsoon system on possibly tectonic timescales.

Key words: Total organic carbon, Carbonate, Opal, Productivity, Sea surface temperature, South China Sea, Monsoon, IMAGES

Citation: Shiau, L. J., P. S. Yu, K. Y. Wei, M. Yamamoto, T. Q. Lee, E. F. Yu, T. H. Fang, and M. T. Chen, 2008: Sea surface temperature, productivity, and terrestrial flux variations of the southeastern South China Sea over the past 800000 years (IMAGES MD972142). Terr. Atmos. Ocean. Sci., 19, 363-376, doi: 10.3319/TAO.2008.19.4.363(IMAGES)

1. INTRODUCTION

The South China Sea (SCS) is the largest marginal sea in the western Pacific. It is characterized by wide continental shelves to the northwest and south, with voluminous run-off from large rivers, and a deep central basin (water depth ~4700 m). The SCS basin is connected to the open ocean through several shallow (~200 to 400 m) gateways, except for the Luzon Strait (~1900 m) in which there is a major channel permitting water exchange from the western Pacific. To the south, the SCS is near the western Pacific warm pool (WPWP), which is considered to be one of the most effective driving engines in the Earth's climate system (Cane 1998; Clement et al. 1999).

The modern climatic patterns of the SCS are primarily

* *Corresponding author*
E-mail: mtchen@mail.ntou.edu.tw

controlled by the East Asian monsoons. The southwest (summer) monsoon lasts from June to September, and brings humid and warm surface air from the south. In the summer monsoon seasons, warm Indian Ocean surface waters flow over the Sunda Shelf into the SCS, resulting in relatively high WPWP sea surface temperatures (SST, ~28°C) in the entire SCS's surface water. During November to March, strong northeast (winter) monsoons from the East Asian continent prevail in the SCS, resulting in a large N-S gradient of SST in the SCS surface water. Strong mixing caused by the winter monsoon winds and cold coastal water intrusion from the north result in high productivity and low SSTs in the northern SCS (Wyrtki 1961; Shaw and Chao 1994).

Previous paleoceanographic studies, based on foraminifer isotopes and fauna assemblages as well as biogenic components from marine sediment cores of the SCS, have concentrated on reconstruction of the climate conditions over the past glacial-interglacial stages (Wang et al. 1995, 1999; Huang et al. 1997a, b; Chen and Huang 1998; Chen et al. 1999; Pelejero et al. 1999a, b). Those studies indicated the dominance of monsoon and/or sea level processes in SCS surface ocean climate variability. Relatively low surface temperatures over the Asian continent in contrast to relatively high temperatures in the western Pacific may have driven stronger northeast monsoons, which induced stronger mixing and greater marine productivity on the surface of the SCS during glacial stages (Chen et al. 2002). The stronger winds may have deepened the mixed layer depth, and also carried large amounts of dust that may have been incorporated into biogenic particles, thereby increasing the transfer rate of organic matter from the sea surface into the deep sea (Ittekkot et al. 1992). Glacial high productivity in the SCS has been supported by the evidence from total organic carbon (TOC), carbonate, and planktic foraminifer fauna assemblage studies (Thunell et al. 1992; Huang et al. 1997a, b). However, the lower sea level during glacial stages gave rise to the emergence of continental shelves and changing bathymetric profiles around the SCS's basin margins (i.e., the Sunda Shelf). During glacial low sea level periods, sediment depositional centers perhaps shifted toward the outer continental shelf and continental slope (Schönfeld and Kudrass 1993). These processes could have brought more fluvial terrestrial sediments to the slope with higher accumulation rates, a condition also favorable for enhanced organic matter preservation in sediments (Müller and Suess 1979; Sarnthein et al. 1988).

In this study, we present a high resolution, long-term reconstruction of SST, productivity, and terrestrial sediment flux variations based on core MD972142 (12°41.133N, 119°27.90N, core length 35.91 m, water depth 1557 m) (Fig. 1a) taken from the southeastern slope of the SCS, near the Palawan Islands during the IMAGES III-IPHIS cruise (Chen et al. 1998). The coring site MD972142 is well above the modern regional lysocline (~3000 m) (Rottman 1979) and carbonate compensation depth (~3800 m) (Thunell et al. 1992), so the core location receives sediments from both SCS marine and Philippine archipelago terrestrial sources, thus it is well-positioned to monitor any variations in marine productivity and terrestrial sediment flux in response to past climate changes. Previous investigations on MD972142 have already established a high precision chronology of the whole length of the record ~870000 years, based on planktic foraminifer oxygen isotopes and AMS ^{14}C dating (Wei et al. 2003) (Fig. 1b), and a preliminary data report on the variations of planktic foraminifer fauna, SSTs, and the TOC and carbonate contents of the past 500000 years (Chen

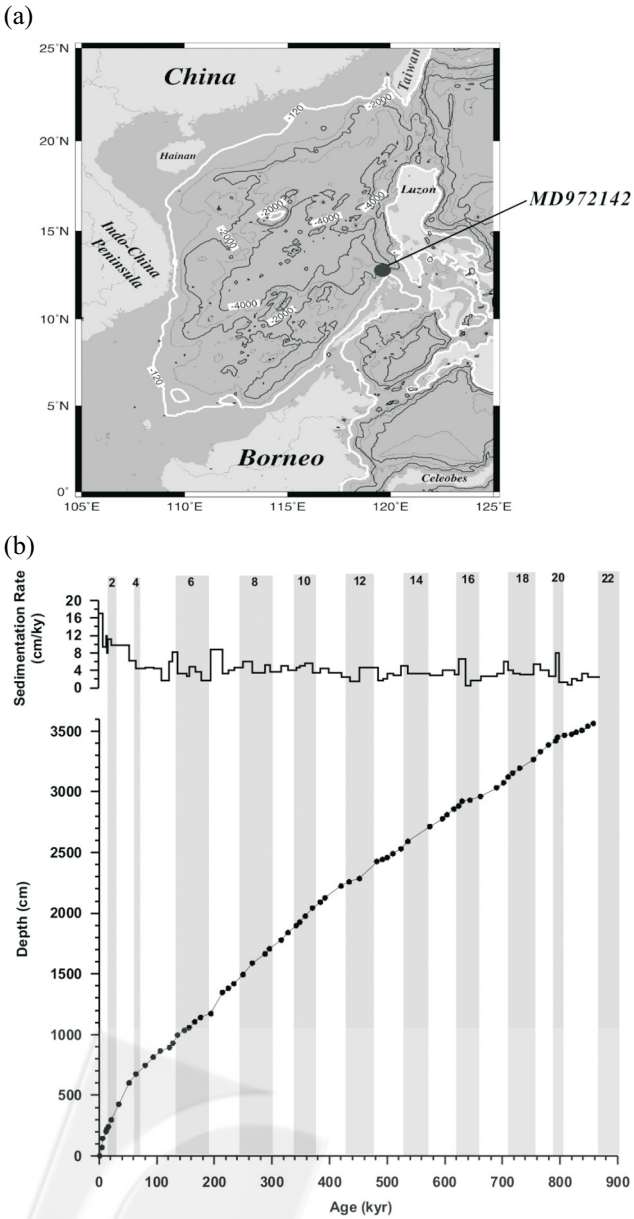

Fig. 1. (a) Location of IMAGES Core MD972142 near the Palawan Islands in the southeastern South China Sea. The white solid line is the estimated coastal line during the glacial periods. (b) The sedimentation rate and age model of core MD972142 (Wei et al. 2003).

et al. 2003). Here we present additional proxy records from MD972142 with an extension to the complete length ~870000 years. We also present analyses of a SST proxy based on an alkenone unsaturation index (Brassell et al. 1986), and various productivity or terrestrial sediment flux proxies: biogenic carbonate, TOC, opal, C_{37} alkenones and n-alkanes contents, and compositions of goethite and hematite derived from color reflectance spectra. In addition to these proxies, composite indices of terrestrial sediment flux (CTI) and of productivity (CPI) were computed and evaluated for their potential as proxies in sediments from this region.

2. DATA AND METHODS

2.1 Biogenic Sediment Contents

We present records of the past ~870000 years based on high resolution sample analyses of core MD972142. This is an extension of our preliminary studies (Chen et al. 2003) which only presented records of the past 500000 years (Chen et al. 2003). Sampling for biogenic component analysis was carried out at 4-cm intervals, and some visible tephra layers were excluded from these analyses. The core length (35.91 m) allowed us to obtain 856 samples for the records, with an average resolution of ~1000 years.

In biogenic component analyses such as those for carbonate, TOC, and opal contents (Fig. 2), we adopted the same procedures as those used in our preliminary studies (Chen et al. 2003). All samples were crushed to a fine powder after drying at 50°C, and split into several sub-samples for analysis of different biogenic components. For the carbonate and TOC analyses, we used a HORIBA EMIA-8210 Carbon Analyzer to determine total carbon (TC). The procedure involves heating the sub-samples at ~1300°C and measuring the combustion product CO_2 gases with an infrared detector. The carbonate contents of the MD972142 core samples were determined by a fuming method (Chang et al. 1991). These sub-samples were reacted with HCl vapor to completely remove all inorganic carbon (TIC) at room temperature for 2 days in an airtight container that contained 100 ml of 12N HCl. After removal of the TIC, the subsamples were measured by the same method using the Carbon Analyzer to determine the TOC contents. The carbonate content can be calculated by subtracting the TOC from the TC values. Replicate analyses of samples for carbonate and TOC contents routinely give an analytical precision of better than 3% by weight. The biogenic opal contents were analyzed by a sodium carbonate leaching method modified from Mortlock and Froelich (1989). The precision based on replicates of the biogenic opal measurement was also within 3% by weight.

2.2 Biomarkers

We analyzed the organic biomarkers from MD972142 sediments for SST, productivity, and terrestrial sediment flux proxies. The SST biomarker we have used is the alkenone-derived $U^{k'}_{37}$ index (Prahl and Wakeham 1987); we calibrated the $U^{K'}_{37}$-SST by using the South China Sea core-top calibration of Pelejero and Grimalt (1997).

The SST estimates of the top samples of core MD972142 range from 28°C to 29°C, which agrees well with the present mean annual SST at this site (Fig. 2). The concordance of core-top estimated and modern observed SSTs argues for the validity of the $U^{k'}_{37}$ method in reconstructing the MD972142 SST record.

C_{37} alkenones are biomarkers synthesized by a group of prymnesiophyte algae, most notably the marine coccolithophorid *Emiliania huxleyi* (Brassell et al. 1986) and *Gephyrocapsa oceanica* (Volkman et al. 1995). The alkenone content is indicative of the level of marine productivity.

The long-chain n-alkanes are synthesized from higher land plants (Eglinton and Hamilton 1967). In this study, we calculated n-alkanes that contain odd carbon numbers from $C_{25} \sim C_{33}$ and used them to monitor the flux of terrestrial organic matter input to the SCS. In the organic biomarkers analyses, we used the solvent dichloromethane: methanol = 6 : 4 to extract the lipids from the freeze-dried sediment samples. After the extraction, we used silica gel column chromatography to separate the alkenones and n-alkanes from the extracts and analyzed those by gas chromatography with flame ionization detection. The detailed procedures were described earlier in Yamamoto et al. (2000).

2.3 Color Spectrum Estimations for Goethite and Hematite

For estimating terrestrial sediment flux variations, we applied a non-destructive, high resolution reflectance method to measure the relative contents of goethite and hematite in core MD972142 sediments. Goethite and hematite are both iron oxide minerals that are products of chemical weathering reactions. In lowland soils, goethite is considered to be favored over hematite with decreasing temperature and increasing precipitation and/or increasing soil organic carbon content (Kämpf and Schwertmann 1983). The presence of small amounts of goethite and/or hematite measurably alters the first derivative spectrum of color reflectance in the visible light range (Deaton and Balsam 1991). Derived from color reflectance spectra, the fraction of goethite in the total iron oxide [G / (G + H)] has therefore been used as a terrestrial precipitation indicator and has been demonstrated to be useful in Amazon Basin sediment studies (Harris and Mix 1999).

We assume that most iron oxide mineral input to the southwestern SCS was from suspended sediment transport by nearby rivers in the Philippine archipelago. The contents of goethite relative to hematite therefore reflect the intensity of chemical weathering or erosion associated with land pre-

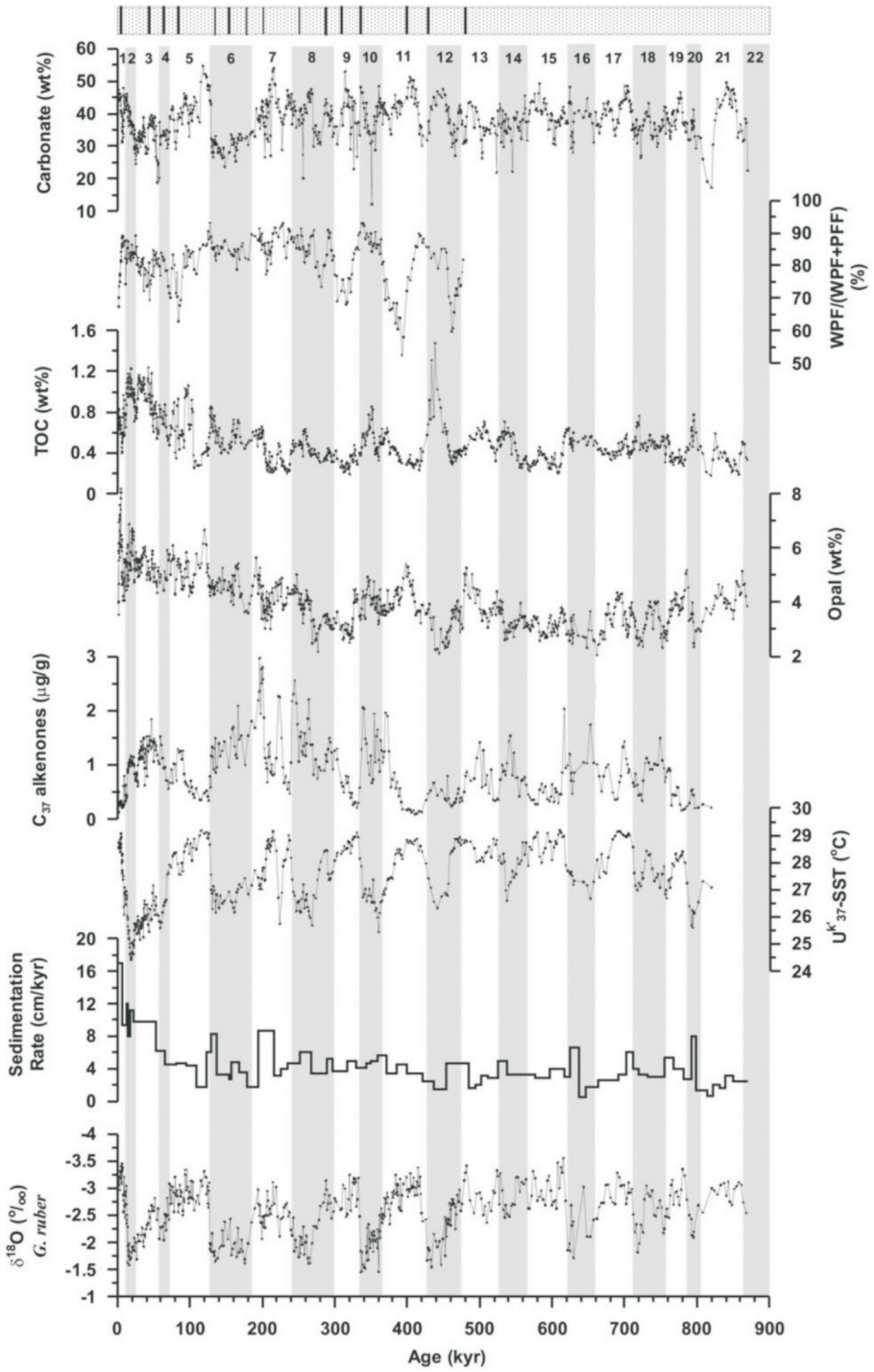

Fig. 2. The down core patterns of carbonate (wt%), preservation of foraminifera [WPF (%): whole planktic foraminifera; PFF: planktic foraminiferal fragments], TOC (wt%), opal (wt%), C_{37} alkenones (μg g^{-1}), $U^{k'}_{37}$-SST (°C), sedimentation rate (cm kyr^{-1}), and $\delta^{18}O$ (*G. ruber*) records of MD972142. The black bars on top indicate the depth of visible tephra layers.

cipitation patterns in the archipelago, which in turn serve as an indicator for variations in riverine terrestrial sediment flux to the southwestern SCS. The color reflectance data of core MD972142 were measured from the wet surfaces of split cores at 2-cm resolution using a Minolta Color Spectrophotometer 2600 in the Laboratory of Earth Environment and Climate Variability at the National Taiwan Ocean University. The procedure for calculating G / G + H (Fig. 3) from MD972142 color reflectance data followed Balsam and Deaton (1991).

2.4 Age Model and Chronology

We used published planktic foraminifer *Globigeri-*

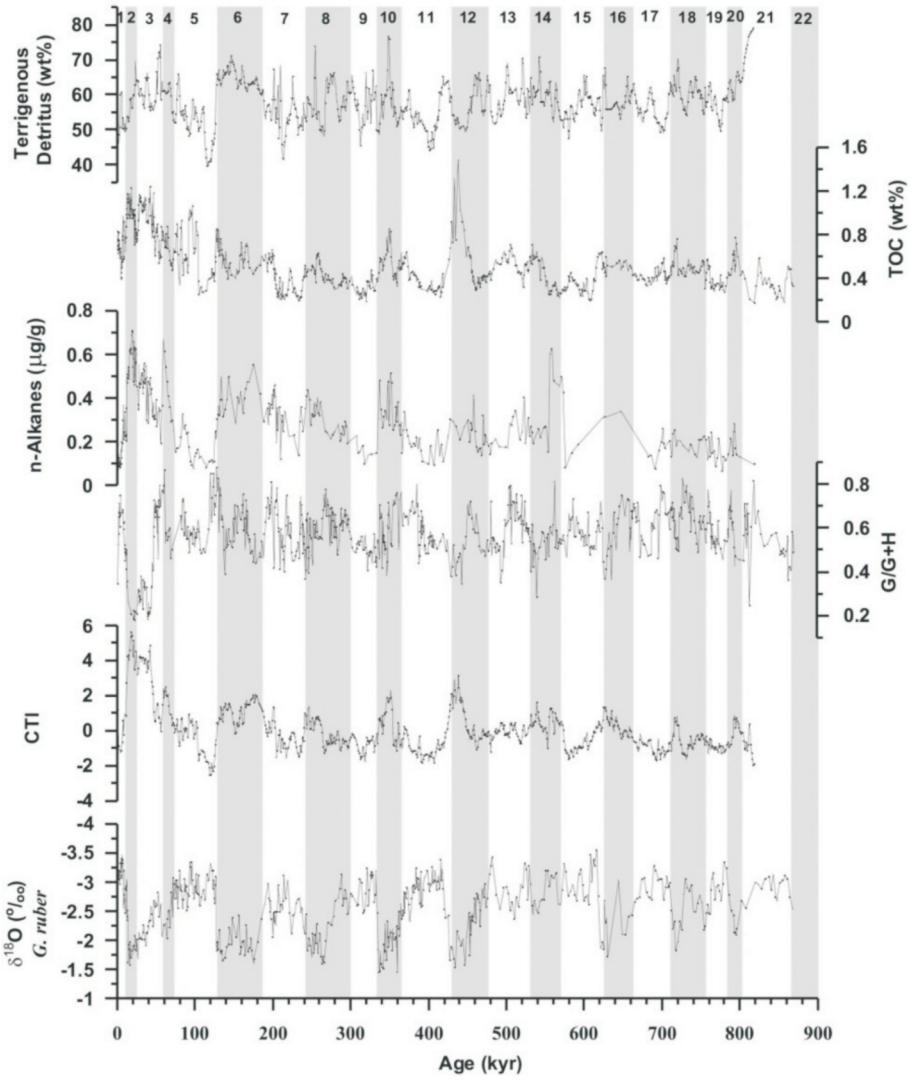

Fig. 3. Terrestrial sediments (wt%), TOC (wt%), n-alkanes (μg g^{-1}), goethite/(goethite+hematite) (G / G + H), CTI, and $\delta^{18}O$ records of MD972142.

noides ruber (white, 250 - 300 μm) oxygen isotope data and age models of core MD972142 (Wei et al. 2003), and a determination of the paleomagnetic reversal Brunhes-Matuyama (Lee 2000) at the bottom of the core to convert our measured proxies from depth to time domains. The oxygen isotope stratigraphy of core MD972142 was established by matching a low latitude stack (Bassinot et al. 1994) with additional AMS ^{14}C dating on samples from the top section of the core.

2.5 Time Series Analysis

We used ARAND programs to calculate the cross-spectra of measured proxy versus oxygen isotope records of core MD972142 for evaluating the coherency and phase relationships between different records in frequency domains with focuses on the three orbital bands: eccentricity (100 kyr^{-1}), obliquity (41 kyr^{-1}), and precession (23 kyr^{-1}). The Blackman-Tukey method of time series analysis (Jenkins and Watts 1968) was used to generate the spectral results. All MD972142 records were interpolated to 1-kyr intervals that correspond to a maximum resolution of 2 kyr (Nyquist period), and 150 lags and bandwidth to 0.0089 were used in estimating the spectra. The value of coherency is the linear correlation coefficient at any frequency in which the spectra align. This program performs a statistical test of the hypothesis that the two time series being analyzed are coherent at a given frequency. The critical value of the statistical test has been set to test for significance at the 80% level.

3. RESULTS

Within the constraints of the oxygen isotope stratigraphic, AMS ^{14}C dating, and paleomagnetic reversal age models, we are able to present time series of planktic foraminifer $\delta^{18}O$, biogenic components in carbonate, TOC, and opal contents, and $U^{k'}_{37}$-SST, C_{37} alkenone and n-alkane contents, color spectra derived abundances of goethite re-

lative to hematite [G / (G + H)], and a planktic foraminifer fragment index for evaluating the carbonate preservation [WPF / (WPF + PFF)] of core MD972142 (Figs. 2, 3). The total length of the records is ~870000 years, and is defined from Marine Isotope Stage (MIS) 1 to MIS 22. Sedimentation rates are ~4 cm kyr^{-1} on average. Relatively high sedimentation rates at the top section of the core are attributed to the stretching of sediments at the top of the giant piston coring system CALYPSO on board the RV *Marine Dufresne* (Széréméta et al. 2004)

The carbonate content makes up ~20 - 50% in weight (Fig. 2). Since the water depth of the core is shallower than the regional lysocline (Thunell et al. 1992), the carbonate pattern observed from MD972142 is presumably driven by productivity and terrestrial sediment dilution. Dissolution and/or preservation should play insignificant roles. We do indeed observe carbonate content maxima corresponding to interglacial stages and minima corresponding to glacial stages (Fig. 2). While comparing this pattern with our preservation index based on foraminifer fragmentation, we found that the carbonate content maxima corresponded to low preservation during most interglacial stages, an impossible relationship if the carbonate content variations are driven by dissolution. We also found carbonate content maxima in some glacial to interglacial transitions (glacial terminations), e.g., in MIS 1/2, 5/6, 7/8, 9/10, and 15/16. In addition, we found several carbonate content minima corresponding to the dilution of the tephra layers visible in core MD972142 (Wei et al. 1998). These layers can be identified with abnormally high magnetic susceptibility (Lee 2000).

TOC contents range from 0.2 to 1.6% in weight (Fig. 2). The TOC content maxima correspond to glacial stages and the minima correspond to interglacial stages. We also found noticeably high TOC contents in MIS 2 - 4, MIS 6, MIS 10, and MIS 12, and during these glacial stages the $U^{k'}_{37}$-SSTs also exhibit a cooling of ~4°C. Besides the orbital-, millennial-scale variability, we observed a long-term increasing trend of TOC contents since ~330 kya, which we assume is related to the longer time scale variability of the late Pleistocene climate.

Opal contents range from 2 to 8% in weight (Fig. 2). Opal content maxima appear to be associated with interglacial stages, although some high contents are found in glacial stages. For example, opal content maxima occur in MIS 1, MIS 2, early and late MIS 5, late MIS 7, MIS 8, MIS 10, MIS 11, late MIS 13, middle MIS 17, and early MIS 19. The opal content pattern appears to be different from that observed in cores from the northern SCS (Chen 1999); this pattern is similar to that observed in the southern SCS (Jian et al. 2000; Wang and Li 2003). More interestingly, we also observed a long-term trend of opal contents increasing since ~330 kya.

The variations of MD972142 $U^{k'}_{37}$-SST between the glacial to interglacial stages are ~3°C. A maximum SST change > 4°C is observed during the Termination I (MIS 2 to MIS 1) (Fig. 2). Consistent with what has been observed in other SST proxies such as Mg/Ca (Cheng 2000) and fauna transform function (Yu et al. 2000) in core MD972142, we found that our $U^{k'}_{37}$-SSTs have a nearly in-phase relationship with $\delta^{18}O$ (Fig. 4). The C_{37} alkenone contents vary from 0.2 to 3 μg g^{-1}. The C_{37} alkenone content is slightly higher in glacial than in interglacial stages (Fig. 2). High C_{37} alkenone contents were recorded from 400 to 130 kya, with the maximum C_{37} alkenone content in late MIS 7. We have observed no long-term trend in the C_{37} alkenone content record. The n-alkane contents vary from 0.1 to 0.7 μg g^{-1} and the contents are higher in glacial than in interglacial stages (Fig. 3). There is a long-term increasing trend of n-alkane content since ~MIS 14.

We evaluated the common effect in all terrestrial sediment flux-related proxies in MD972142: terrigenous detritus (100% - total biogenic components%), TOC, n-alkanes, and goethite / (goethite + hematite) [G / (G + H)] (Fig. 3). Visual inspection of these four proxy records shows some similar time intervals of increased terrestrial input, indicating a common effect attributable to terrestrial influences. For example, in the broad time intervals of early MIS 5, middle MIS 6, MIS 8, MIS 10, and late MIS 11, these proxies suggest high terrestrial input. It appears that the four proxy records are linked to terrestrial input variations but are complicated by other processes such as differential preservation, biological productivity, and/or oceanographic processes particular to the individual proxy. To evaluate a common effect that is more directly linked to terrestrial input, we assessed the variance in common among the four proxy records by extracting the first principal component from the records using a principal component analysis (PCA). We first interpolated each record to a common 1000-yr sample interval (the average time resolution of the records), and standardized each to unit variance. The first component, which we called a composite terrestrial index (CTI), indicates that 40% of the total variance in the four records is explained by a common effect which is related to variations in terrestrial sediment flux (Table 1). The high CTI values, as observed from a R-mode matrix of the PCA, correlate positively with TOC and the n-alkane content, and coincide with most maximum glacial stages, which suggests that glacial boundary conditions are important in driving more terrestrial sediment input to core MD972142.

We also evaluated the common effect in all productivity-related proxies in MD972142: carbonate, TOC, opal and C_{37} alkenone contents (Fig. 4). With the same statistical procedure used in extracting CTI, we used PCA to extract the first component, called the composite productivity index (CPI), which explains 37% of the total variance in the four records (Table 2). The high CPI values correlate positively with TOC, opal, and C_{37} alkenone content, and apparently reach maxima in late glacial stages (Fig. 4). High CPI values

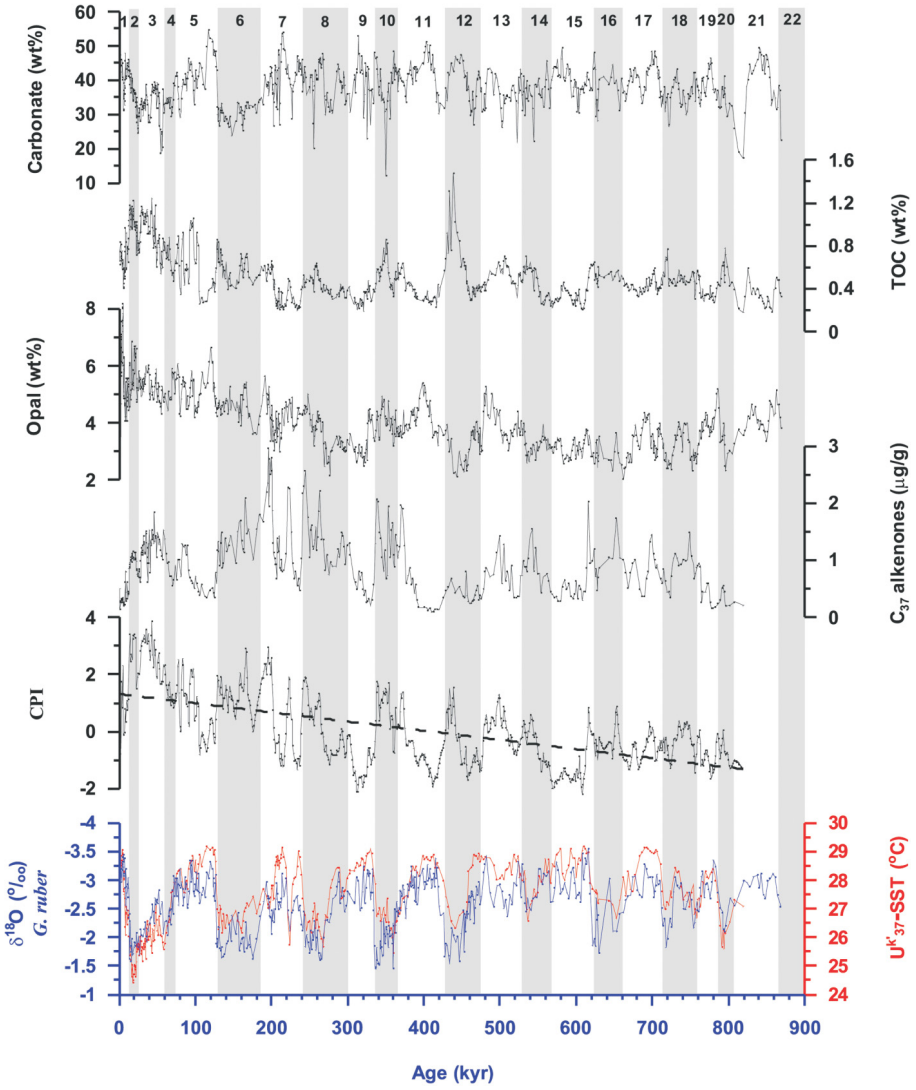

Fig. 4. Carbonate (wt%), TOC (wt%), opal (wt%), C_{37} alkenones (μg g^{-1}), CPI, U-SST (°C), and $\delta^{18}O$ records of MD972142. The dashed line indicates a long-term trend of increased productivity since the middle Pleistocene. The $U^{k'}_{37}$-SST (red line) and $\delta^{18}O$ (blue line) variations show nearly in-phase relationships.

Table 1. R-mode principle component analysis for composite terrestrial index (CTI).

Terrestrial Sediment indices	PC 1 (CTI)	PC 2	PC 3	PC 4
Terrigenous detritus	0.205	0.911	-0.251	0.254
TOC	0.610	-0.247	0.300	0.691
n-Alkanes	0.605	0.162	0.419	-0.657
G / G + H	-0.470	0.287	0.819	0.161
Variance	0.401	0.254	0.204	0.141

coincide with low $U^{k'}_{37}$-SSTs, and exhibit a long-term trend of increased productivity since the middle Pleistocene (Fig. 4), suggesting that glacial boundary conditions are also important in explaining the timing of productivity variations. The long-term productivity change observed in our record appears to link with climate mechanisms operating on much longer, possibly tectonic timescales.

Cross-spectra analyses of the MD972142 records provide evaluation on more precise amplitude and timing of the complex variations shown in various proxies on frequency domains. The CTI record clearly shows peak periods close to all orbital periods (100, 41, and 23 kyr^{-1} bands),

which in turn exhibits statistically significant coherence (80% confidence level) with the oxygen isotope record. Phase spectra analysis indicates that the orbital frequencies in the CTI maxima are nearly in-phase with the ice volume maxima (Fig. 5). The CPI record shows complex spectra mixed with orbital-related and non-orbital periods

Table 2. R-mode principle component analysis for composite productivity index (CPI).

Productivity-related indices	PC 1 (CPI)	PC 2	PC 3	PC 4
Carbonate	-0.172	0.966	-0.142	0.128
TOC	0.625	0.016	0.053	0.779
Opal	0.540	0.255	0.641	-0.482
C_{37} alkenones	0.537	0.035	-0.752	-0.380
Variance	0.376	0.248	0.206	0.169

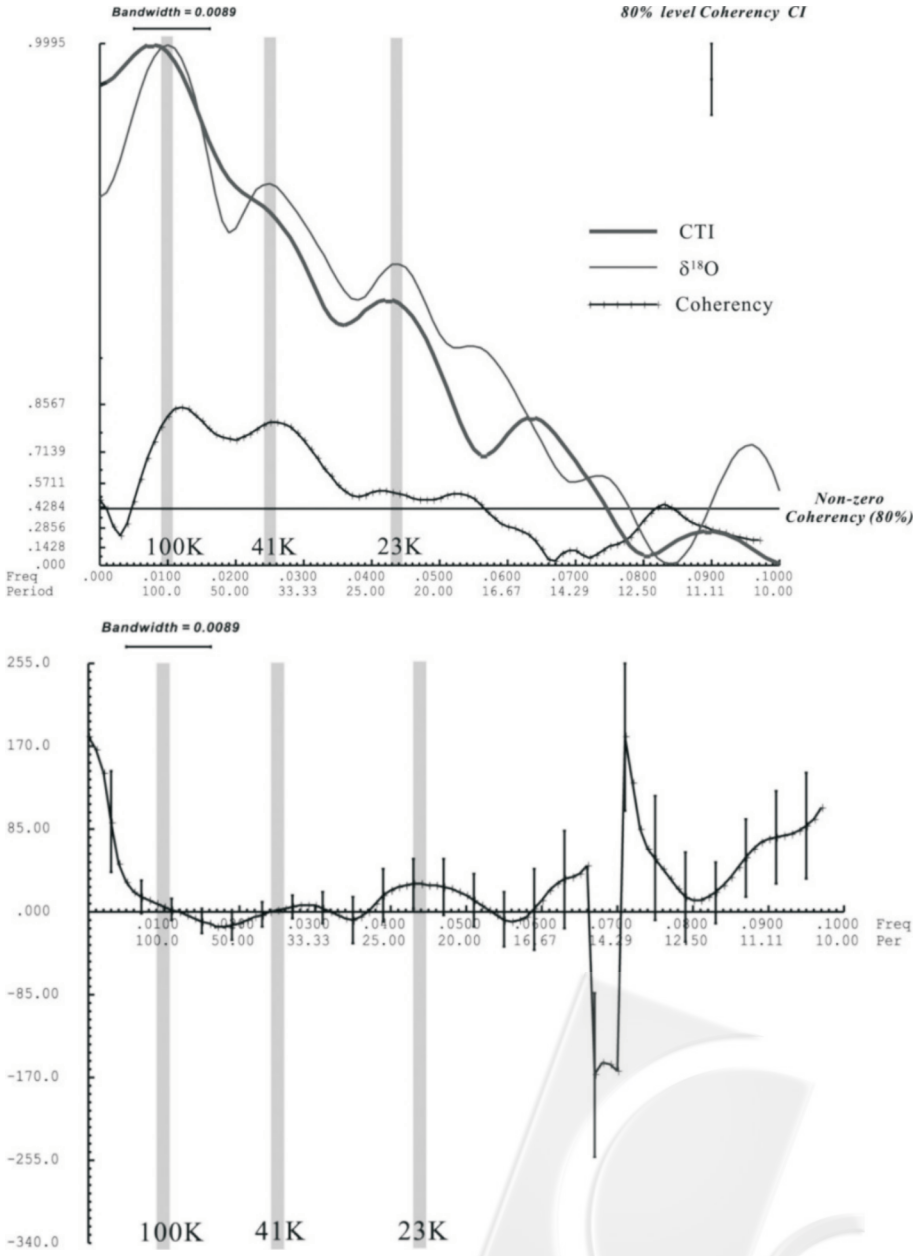

Fig. 5. Cross-spectral analyses between CTI and the oxygen isotope records of MD972142. (N = 819, lags = 150, *BW* = 0.0089, Δt = 1 kyr).

(54 and 29 kyr^{-1}), but statistically significant coherence (80% confidence level) is only observed on the frequency bands from 100 to 41 kyr^{-1}. The phase spectra indicate the CPI maxima have nearly in-phase relationships with the ice volume maxima on the 100 kyr^{-1} frequency, but lag significantly (~50°) the ice volume maxima on the 41 kyr^{-1} frequency band (Fig. 6). Our cross-spectral analyses suggest the importance of glacial boundary conditions in determining the amplitude and timing of terrestrial sediment flux and productivity variations in core MD972142.

4. DISCUSSION

4.1 Terrestrial Sediment Flux Variations

Cyclical fluctuations in carbonate records are common features of pelagic and hemipelagic marine sediments deposited during the Quaternary. Carbonate content variations in marine sediments are controlled by three main processes: marine carbonate productivity, carbonate dissolution, and dilution of non-biogenic carbonate, such as terrestrial, eolian and volcanic particles, and biogenic siliceous particles (Volat et al. 1980). The variations in MD972142 carbonate contents show a pattern similar to that reported by many previous studies in the SCS (Thunell et al. 1992; Wang et al. 1995; Chen et al. 1997; Chen and Huang 1998; Chen et al. 1999). All these previous studies suggest that the first order variations shown in the SCS carbonate records reflect changes in terrestrial sediment input in past glacial and interglacial cycles.

Productivity changes appear to be unimportant in con-

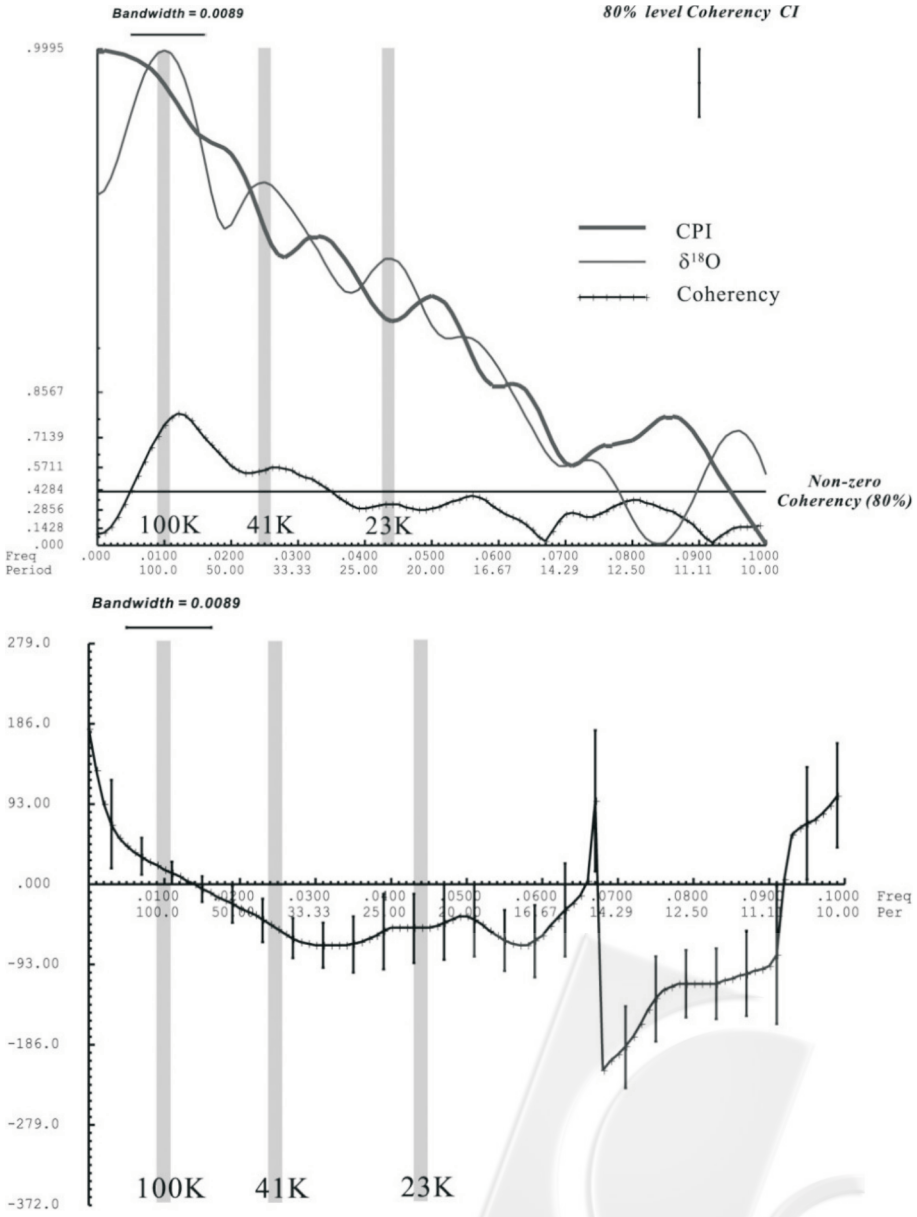

Fig. 6. Cross-spectral analyses between CPI and the oxygen isotope records of MD972142. (N = 819, lags = 150, *BW* = 0.0089, Δt = 1 kyr).

trolling the MD972142 carbonate records. While comparing C_{37} alkenone content, one of the indicators related to carbonate productivity (Kennedy and Brassell 1992), to carbonate contents in MD972142 (Fig. 2), we found high carbonate productivity is associated with low carbonate content, an impossible relationship for attributing productivity as the main variable driving carbonate content changes. In addition, glacial carbonate preservation is considered to be relatively better than that in interglacial stages in the Pacific (Le and Shackleton 1992), as evidenced by foraminifer fragmentation analysis on core MD972142 (Fig. 2). Carbonate preservation does not appear to be responsible for driving carbonate content changes in MD972142.

We attribute the carbonate content variations in MD 972142 to changes in terrestrial sediment flux in the SCS. During glacial low sea levels, large areas of the continental shelves in the SCS was exposed, which in turn resulted in more terrestrial sediments deposited on the shelves being transported to the deep sea. In addition, during glacial low sea levels, the river mouths around the SCS were closer to the site of MD972142, thus more terrestrial sediment fluxes were received. Increased n-alkane contents in glacial stages (Fig. 3) support the attribution of dilution effects of terrestrial sediment flux on carbonate changes in MD972142. Our cross-spectra analysis on CTI versus the oxygen isotope record in MD972142 also consistently suggests that the terrestrial sediment inputs reach maxima during global ice volume maxima (low sea level) in MD972142, implying a direct link between terrestrial sediment flux and sea level fluctuations in the SCS.

4.2 Productivity and Monsoon Variations

TOC contents are often used as productivity indicators in marine sediment studies. Our MD972142 TOC contents are high during glacial stages and low in interglacial stages, suggesting a pattern of productivity change similar to that observed in previous studies (Thunell et al. 1992). TOC content variations are controlled by marine biological productivity, the preservation of organic matter (affected by a redox environment in the deep sea or by sedimentation rate), and terrestrial organic matter input. Glacial high TOC contents in the SCS are postulated to occur in response to the intensification of East Asian winter monsoons, which increases the mixing and upwelling in surface waters, which in turn increases productivity in the SCS (Huang et al. 1997a, b). The C/N ratio of organic matter in SCS sediments also indicates that the TOC is mainly marine in origin (Thunell et al. 1992), also suggesting increased productivity due to stronger monsoons. To identify different origins of the organic matter in MD972142 sediments, we have measured the $\delta^{13}C_{org}$ for sediments showing high TOC contents (MIS 2, MIS 10, and MIS 12) (not shown). The $\delta^{13}C_{org}$ data vary from -21‰ (MIS 12) to -18‰ (MIS 2) (Löwemark et al. 2005). The $\delta^{13}C_{org}$ values of marine algae vary from -20‰ to -22‰. On land, the $\delta^{13}C_{org}$ values of C_3 plants (such as trees, shrubs, and cool-climate grasses) are ~-27‰, and C_4 plants are ~-14‰ (Meyers 1997). Our $\delta^{13}C_{org}$ values suggest that the organic matter in core MD 972142 is mostly marine in origin, although at this stage it is difficult to rule out the possibility that C_4 plants on land contributed more organic matter to the SCS during glacial low sea level conditions.

Preservation is also an important factor in determining the contents of TOC in marine sediments. Increased terrestrial sediment input to core MD972142 is observed in glacial stages based on our CTI values (Fig. 3). Although the first order, low frequency variations in the MD972142 TOC content appear to be mainly affected by changes in the terrestrial sediment input – which is consequently related to global sea level fluctuations, regional precipitation patterns and riverine transport, some short-lived, high frequency TOC content changes (i.e., in MIS 2 - 4, MIS 6, MIS 10, and MIS 12) do not coincide with high sedimentation rates in core MD972142 (Fig. 2). In contrast, these high TOC contents in MD972142 link more closely to major cooling in the surface water of the SCS, as evidenced by our U^{K}_{37}-SST estimates (Fig. 2). This relationship suggests that changes in productivity in MD972142 occurred in response to surface ocean cooling caused by stronger mixing, which reflects primarily winter monsoon forcing in the SCS.

While comparing our MD972142 CPI record to other monsoon productivity records from the Indian and western Pacific Oceans (Fig. 7) (i.e., Arabian Sea productivity record KL15 at 12°51.5'N, 47°25.90'E, by Almogi-Labin et al. 2000), we found high similarity among those records from more regional scales. Especially notable is the fact that all these monsoon productivity records show several short-lived high productivity events in MIS 2 - 4, MIS 6, MIS 10, and MIS 12 (Fig. 7). The regionally consistent pattern of high productivity intervals also lends credence to our attribution of the high productivity observed in MD 972142 to increased winter monsoon wind strength in East Asia.

Biogenic opal is an indicator for marine productivity produced by siliceous organisms such as diatoms or radiolarians (e.g., Sarnthein et al. 1988; Mortlock et al. 1991). Sediment trap experiments (Wiesner et al. 1996) indicate that the opal flux is mainly controlled by summer monsoon winds in the southern SCS. Our opal content record in MD972142 is high in most interglacial stages, the same pattern that has been previously reported from SONNE core 17957 (10°53.9'N, 115°18.30'E) (Jian et al. 2000) in the southern SCS. In addition, the opal record of MD972142 is well correlated with an Arabian summer monsoon TOC record from ODP site 723 (18°03.079'N, 57°36.561'E) (Emeis et al. 1995). Basically, nutrients for siliceous organism growth could be supplied by river plumes (Schneider et al.

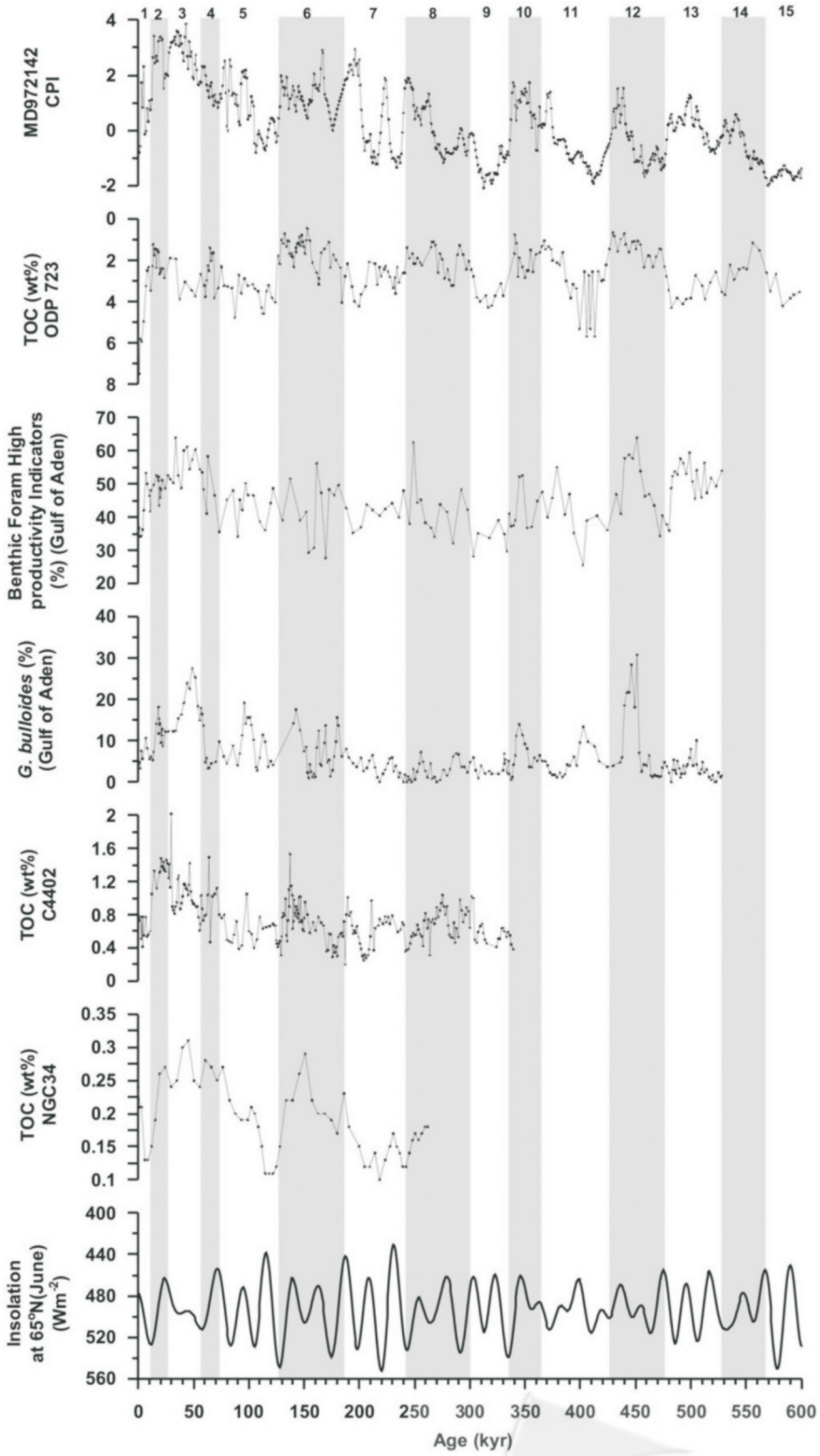

Fig. 7. MD972142 CPI record comparing the TOC (wt%) record from ODP site 723 (Emeis et al. 1995), the productivity record of benthic foram high productivity indicators (%) and *G. bulloides* (%) from KL15 (Almogi-Labin et al. 2000), the TOC (wt%) records from the WPWP (C4402: Kawahata et al. 1998; NGC34: Kawahata and Eguchi 1996), and insolation at 65°N in June.

1997). Increased precipitation during summer monsoon periods in the Philippine and Palawan Islands results in more nutrients being brought into the ocean by rivers, which in turn supports high siliceous productivity. Our MD972142 goethite abundances relative to hematite [G / (G + H)] clearly show some high values in interglacial stages (Fig. 3),

implying relatively warm and humid climate conditions that increase precipitation and river runoff to the SCS.

4.3 Long-term Climate Evolution in the Late Pleistocene

The long-term trend of increased TOC, opal, and CPI records with decreased $U^{k'}_{37}$-SSTs in MD972142 is noteworthy. This trend is particularly pronounced after ~330 kya. The same long-term change of thermocline depth shoaling since the late Pleistocene has been reported from SONNE core 17957 in the southern SCS (Jian et al. 2000), and was attributed to a strengthened East Asian monsoon system resulting from the uplift of the Tibetan Plateau (Jian et al. 2000). The stronger East Asian monsoon system may also impact hydrographic conditions in the SCS, especially since a globally reported Mid-Brunhes event after ~400 kya (Jansen et al. 1986), which may be associated with the southward migration of the polar front in the Southern Ocean (Jansen et al. 1986). In previous studies of the Southern Ocean, there is a large southward migration of the polar front since ~400 kya (Becquey and Gersonde 2002), which may result in stronger oceanic circulation on a global scale. Records from ODP site 1123 (41°47.2'S, 171°29.9'E) (Hall et al. 2001) in the Southern Ocean also show an increased trend of bottom current strength. The long-term increases in productivity and decline in SSTs might reflect ocean circulation changes operating on longer, possibly tectonic timescales. The evaluation of biogenic or organic matter preservation or diagenesis imprints on the long-term trends, however, awaits future study.

5. CONCLUSIONS

We have presented a detailed record ~870000 years long of the biogenic components (carbonate, TOC, and opal), $U^{k'}_{37}$-SST, C_{37} alkenone and n-alkane contents, and color spectra estimates of goethite abundances relative to hematite from a southeastern SCS core (MD972142). The following conclusions can be draw from analysis of these records:

1. Over the entire length of the record, the interglacial stages are characterized by relatively high carbonate and opal, but low TOC contents, and the glacial stages are characterized by low carbonate and opal, and high TOC contents. The carbonate content variations are attributed to changes in terrestrial sediment input in response to sea level fluctuations. The TOC content variations may reflect a combination of factors related to both winter monsoon-driven productivity and terrestrial sediment flux. The opal content variations are controlled mainly by siliceous productivity related to summer monsoon strength and regional precipitation, as well as riverine input of nutrients;
2. A composite terrestrial index (CTI) and composite productivity index (CPI) were constructed for the MD972142 records through a principal component analysis of a suite of the sediment proxies that are sensitive to terrestrial sediment input or productivity. The maxima of the CTI and CPI values coincide with global ice volume maxima. Cross-spectra analyses of the CTI and CPI against the MD972142 foraminifer $\delta^{18}O$ record indicate nearly in-phase relationships over three orbital frequency bands, suggesting that the glacial boundary conditions play important roles in determining the amplitude and timing of SCS climate variability;
3. We have observed long-term trends of increased productivity and decreased SST in the MD972142 records. These long-term trends are robustly-expressed in productivity-related proxies and are more pronounced since the mid-Brunhes, from ~330 kya. The long-term trends observed in this study are most likely attributable to changes in SCS hydrography, productivity, and/or preservation associated with increased strength of the East Asian monsoon system on possibly tectonic timescales.

Acknowledgements We thank two anomalous reviewers for their comments and helpful reviews. We also thank Dr. S. J. Kao at the Research Center for Environmental Changes at the Academia Sinica for helping to analyze the $\delta^{13}C_{org}$ data. Ms. C. H. Chu helped analyze the color reflectance data. Members who work in the Core Repository and Laboratory at the National Center for Ocean Research (NCOR) are also due our thanks for helping us finish the measurements in this study. This research was supported by the National Science Council (NSC95-2611-M-019-012 & NSC95-2611-M-019-013) and National Taiwan Ocean University, Republic of China.

REFERENCES

Almogi-Labin, A., G. Schmiedl, C. Hemleben, R. Siman-Tov, M. Segl, and D. Meischner, 2000: The influence of the NE winter monsoon on productivity changes in the Gulf of Aden, NW Arabian Sea, during the last 530 ka as recorded by foraminifera. *Mar. Micropaleontol.*, **40**, 295-319.

Balsam, W. L. and B. C. Deaton, 1991: Sediment dispersal in the Atlantic Ocean: Evaluation by visible light spectra. *Rev. Aquatic Sci.,* **4**, 411-447.

Bassinot, F. C., L. D. Labeyrie, E. Vincent, X. Quidelleur, N. J. Shackleton, and Y. Lancelot, 1994: The astronomical theory of climate and the age of the Brunches-Matuyama magnetic reversal. *Earth Planet. Sci. Lett.*, **126**, 91-108.

Becquey, S. and R. Gersonde, 2002: Past hydrographic and climatic changes in the Subantarctic Zone of the South Atlantic-The Pleistocene record from ODP Site 1090. *Palaeogeogr. Palaeoclimatol. Palaeoecol.*, **182**, 221-239.

Brassell, S. C., G. Eglinton, I. T. Marlowe, U. Pflaumann, and M. Sarnthein, 1986: Molecular stratigraphy: A new tool for climatic assessment. *Nature*, **320**, 129-133.

Cane, M., 1998: Climate change: A role for the Tropical Pacific. *Science*, **282**, 59-61.

Chang, F. Y., S. J. Kao, and K. K. Liu, 1991: Analysis of organic and carbonate in sediments. *Acta Oceanogr. Taiwan.*, **27**, 140-150. (in Chinese)

Chen, M. T. and C. Y. Huang, 1998: Ice-volume forcing of winter monsoon climate in the South China Sea. *Paleoceanography,* **13**, 622-633.

Chen, M. T., C. Y. Huang, and K. Y. Wei, 1997: 25,000-years late Quaternary records of carbonate preservation in the South China Sea. *Palaeogeogr. Palaeoclimatol. Palaeoecol.,* **129**, 155-169.

Chen, M. T., L. Beaufort, and the Shipboard Scientific Party of the Images III/MD106-IPHIS Cruise (Leg II) 1998: Exploring Quaternary variability of the East Asia monsoon, Kuroshio Current, and Western Pacific Pool system: High resolution investigations of paleoceanography from the IMAGES III (MD106)-IPHIS Cruise. *Terr. Atmos. Ocean. Sci.,* **9**, 129-142.

Chen, M. T., C. H. Wang, C. Y. Huang, L. Wang, and M. Sarnthein, 1999: A late Quaternary planktonic foraminifer faunal record of rapid climatic changes from the South China Sea. *Mar. Geol.*, **156**, 85-108.

Chen, M. T., Y. Y. Chen, T. S. Fang, C. Y. Huang, and T. Q. Lee, 2002: The structure of the last deglaciation in South China Sea high-resolution records: IMAGES core MD972148. In: Chen, C. T. A. (Ed.), Marine Environment: The Past, Present, and Future, The Fuwen Press, Kaohsiung, Taiwan, 79-94.

Chen, M. T., L. J. Shiau, P. S. Yu, T. C. Chiu, Y. G. Chen, and K. Y. Wei, 2003: 500,000-year records of carbonate, organic carbon, and foraminiferal sea-surface temperature from the southeastern South China Sea (Near Palawan Island). *Palaeogeogr. Palaeoclimatol. Palaeoecol.*, **197**, 113-131.

Chen, Y. Y., 1999: Late Quaternary paleoclimate record of biogenic sediment from the South China Sea. Master Thesis, Institute of Applied Geophysics, National Taiwan Ocean University, Keelung, Taiwan, 105 pp.

Cheng, Y. Y., 2000: Reconstruction of paleotemperature and paleosalinity of the South China Sea for the past 170 kyrs using planktonic foraminiferal Mg/Ca ratio and isotopes. Master Thesis, Institute of Geosciences, National Taiwan University, Taipei, Taiwn, 66 pp.

Clement, A. C., R. Seager, and M. A. Cane, 1999: Orbital controls on the El Niño/Southern Oscillation and the tropical climate. *Paleoceanography*, **14**, 441-456.

Deaton, B. C. and W. L. Balsam, 1991: Visible Spectroscopy-A rapid method for determining hematite and goethite concentration in geological materials. *J. Sediment. Petrol.*, **61**, 628-632.

Eglinton, G. and R. J. Hamilton, 1967: Leaf epicuticular waxes. *Science*, **156**, 1322-1335.

Emeis, K. C., D. M. Anderson, H. Doose, D. Kroon, and D. Schulz-Bull, 1995: Sea-surface temperatures and the history of monsoon upwelling in the northwest Arabian Sea during the last 500,000 years. *Quat. Res,* **43**, 355-361.

Hall, I. R., N. McCave, N. J. Shackleton, G. P. Weedon, and S. E. Harris, 2001: Intensified deep Pacific inflow and ventilation in Pleistocene glacial times. *Nature*, **412**, 809-812.

Harris, S. E. and A. C. Mix, 1999: Pleistocene precipitation balance in the Amazon basin recorded in deep sea sediments. *Quat. Res.*, **51**, 14-26.

Huang, C. Y., P. M. Liew, M. Zhao, T. C. Chang, C. M. Kuo, M. T. Chen, C. H. Wang, and L. F. Zheng, 1997a: Deep sea and lake records of the Southeast Asian paleomonsoons for the last 25 kyrs. *Earth Planet. Sci. Lett.*, **146**, 59-72.

Huang, C. Y., S. F. Wu, M. Zhao, M. T. Chen, C. H. Wang, X. Tu, and P. B. Yuan, 1997b: Surface ocean and monsoon climate variability in the South China Sea since last glaciation. *Mar. Micropaleontol.,* **32**, 71-94.

Ittekkot, V., B. Haake, M. Bartsch, R. R. Nair, and V. Ramaswamy, 1992: Organic carbon removal in the sea: The continental connection. In: Summerhayes, C. P., W. L. Prell, and K. C. Emeis (Eds.), Upwelling Systems: Evolution Since the Early Miocene, Geological Society Special Publication, **64**, 167-176.

Jansen, J. H. F., A. Kuijpers, and S. R. Troelstra, 1986: A Mid-Brunhes climatic event: Long-term changes in global atmosphere and ocean circulation. *Science*, **232**, 619-622.

Jenkins, G. M. and D. G. Watts, 1968: Spectral analysis and its applications. Holden-Day, San Fransico, 525 pp.

Jian, Z., P. Wang, M. P. Chen, B. Li, Q. Zhao, C. Buhring, C. Laj, H. L. Lin, U. Pflaumann, Y. Bian, R. Wang, and X. Cheng, 2000: Foraminiferal responses to major Pleistocene paleoceanographic changes on the southern South China Sea. *Paleoceanography*, **15**, 229-243.

Kämpf, N. and U. Schwertmann, 1983: Goethite and hematite in a climosequence in southern Brazil and their application in classification of kaolinitic soils. *Geoderma*, **29**, 27-39.

Kawahata, H. and N. Eguchi, 1996: Biogenic sediments on the Eauripik Rise of the west equatorial Pacific during the late Pleistocene. *Geochem. J.*, **30**, 201-215.

Kawahata, H., N. Suzuki, and N. Ahagon, 1998: Biogenic sediments in the West Caroline Basin, the western equatorial Pacific during the last 330,000 years. *Mar. Geol.*, **149**, 155-176.

Kennedy, J. A. and S. C. Brassell, 1992: Molecular records of twentieth-century El Niño events in laminated sediments from the Santa Barbara Basin. *Nature*, **357**, 62-64.

Le, J. and N. J. Shackleton, 1992: Carbonate dissolution fluctuations in the western equatorial Pacific during the Quaternary. *Paleoceanography*, **7**, 21-42.

Lee, T. Q., 2000: Geomagnetic secular variation of the last one million years recorded in Core MD972142 from the Southeastern South China Sea. *J. Geol. Soc. China*, **43**, 423-434.

Löwemark, L. A., K. Y. Wei, C. H. Wang, C. Y. Lee, S. R. Song, M. T. Chen, L. J. Shiau, H. S. Mii, S. Steinke, H. L. Lin, and S. J. Kao, 2005: Orbital-Scale Variability of Deep-Water Circulation in the South China Sea, EOS Trans. AGU, **86**, Fall Meet. Suppl., Abstract pp11B-1463.

Meyers, P. A., 1997: Organic geochemical proxies of paleoceanographic, paleolimnologic, and paleoclimatic processes. *Org. Geochem.*, **27**, 213-250.

Mortlock, R. A. and P. N. Froelich, 1989: A simple method for the rapid determination of biogenic opal in pelagic marine sediments. *Deep-Sea Res.*, **36**, 1415-1429.

Mortlock, R. A., C. D. Charles, P. N. Forelich, M. A. Ziberllo, J. Saltzman, J. D. Hays, and L. H. Burkle, 1991: Evidence for low productivity in the Antarctic Ocean during the last glaciation. *Nature*, **351**, 220-223.

Müller, P. J. and E. Suess, 1979: Productivity, sedimentary rate and sedimentary organic matter in the ocean I. Organic carbon preservation. *Deep-Sea Res*., **26**, 1347-1362.

Pelejero, C. and J. O. Grimalt, 1997: The correlation between the U^k_{37} index and the sea surface temperatures in the warm boundary, the South China Sea. *Geochim. Cosmochim. Acta*, **61**, 4789-4797.

Pelejero, C., J. O. Grimalt, M. Sarnthein, L. Wang, and J. A. Flores, 1999a: Molecular biomarker record of sea surface temperature and climatic change in the South China Sea during the last 140,000 years. *Mar. Geol.*, **156**, 109-121.

Pelejero, C., J. O. Grimalt, S. Heilig, M. Kineast, and L. Wang, 1999b: High-resolution U^k_{37} temperature reconstruction in the South China Sea over the past 220 kyr. *Paleoceanography*, **11**, 15-35.

Prahl, F. G. and S. G. Wakeham, 1987: Calibration of unsaturation patterns in long-chain ketone compositions for palaeotemperature assessment. *Nature*, **330**, 367-369.

Rottman, M. L., 1979: Dissolution of planktonic foraminifera and pteropods in the South China Sea sediments. *J. Foraminiferal Res.*, **9**, 41-49.

Sarnthein, M., K. Winn, J. C. Duplessy, and M. R. Fontugne, 1988: Global variations of surface ocean productivity in low and mid latitudes: Influence on CO_2 reserviors of the deep ocean and atmosphere during the last 21,000 years. *Paleoceanography*, **3**, 361-399.

Schneider, R., B. Price, P. J. Müller, D. Kroon, and I. Alexander, 1997: Monsoon related variations in Zarie (Congo) sediment load and influence of fluvial silicate supply on marine productivity in the east equatorial Atlantic during the last 200,000 years. *Paleoceanography*, **12**, 463-481.

Schönfeld, J. and H. R. Kudrass, 1993: Hemipelagic sediment accumulation rates in the South China Sea related to late Quaternary sea-level changes. *Quat. Res.*, **40**, 368-379.

Shaw, P. T. and S. Y. Chao, 1994: Surface Circulation in the South China Sea. *Deep-Sea Res. I*, **41**, 1663-1683.

Széréméta, N., F. Bassinot, Y. Bault, L. Labeyrie, and M. Pagel, 2004: Oversampling of sedimentary series collected by giant piston corer: Evidence and corrections based on 3.5-kHz chirp profiles. *Paleoceanography*, **19**, PA1005, doi: 10.1029/2002PA000795.

Thunell, R. C., Q. Miao, S. E. Calvert, and T. F. Pedersen, 1992: Glacial-Holocene biogenic sedimentation patterns in the South China Sea: Productivity variations and surface water pCO_2. *Paleoceanography*, **7**, 143-162.

Volat, J. L., L. Pastouret, and V. Vergnaud-grazzini, 1980: Dissolution and carbonate fluctuations in Pleistocene deep-sea cores: A review. *Mar. Geol.*, **34**, 1-28.

Volkman, J. K., S. M. Barrerr, S. I. Blackburn, and E. L. Sikes, 1995: Alkenones in Gephyrocapsa oceanica: Implications for studies of paleoclimate. *Geochim. Cosmochim. Acta*, **59**, 513-520.

Wang, L., M. Sarnthein, H. Erlenkeuser, J. Grimalt, P. Grootes, S. Heilig, E. Ivanova, M. Kienast, C. Pelejero, and U. Pflaumann, 1999: East Asia monsoon climate during the late Pleistocene: High-resolution sediment records from the South China Sea. *Mar. Geol.*, **156**, 245-284.

Wang, P., L. Wang, Y. Bian, and Z. Jian, 1995: Late Quaternary paleoceanography of the South China Sea: Surface circulation and carbonate cycles. *Mar. Geol.*, **127**, 145-165.

Wang, R. and J. Li, 2003: Quaternary high-resolution opal record and its paleoproductivity implications at ODP Site 1143, southern South China Sea. *Chin. Sci. Bull.*, **48**, 363-367.

Wei, K. Y., T. Q. Lee, and the Shipboard Scientific Party of the Images III/MD106-IPHIS Cruise (Leg II), 1998: Late Pleistocene volcanic ash layers in Core MD972142, offshore from northwestern Palawan, South China Sea: A preliminary report. *Terr. Atmos. Ocean. Sci.*, **9**, 143-152.

Wei, K. Y., T. C. Chiu, and Y. G. Chen, 2003: Toward establishing a maritime proxy record of the East Asian summer monsoons for the late Quaternary. *Mar. Geol.* **201**, 67-79.

Wiesner, M. G., L. Zheng, H. K. Wong, Y. Wang, and W. Chen, 1996: Fluxes of particulate matter in the South China Sea. In: Ittekkot, V., P. Schafer, S. Honjo, and P. J. Depetris (Eds.), Particle Flux in the Ocean, John Wiley & Sons Ltd., 293-312.

Wyrtki, K., 1961: Physical oceanography of the southeast Asian waters: Scientific results of maritime investigations of the South China Sea and the Gulf of Thailand 1959 - 1961, Naga Report, 2, Scripps Institution of Oceanography, La Jolla, California.

Yamamoto, M., M. Yamamuro, and R. Tada, 2000: Late Quaternary records of organic carbon, calcium carbonate, and biomarkers from site 1016 off Point Conception, California margin. In: Lyle, M., I. Koizumi, C. Richter, and T. C. Moore, jr. (Eds.), *Proc. ODP, Sci. Results,* **167**, College Station, TX (Ocean Drilling Program), 183-194.

Yu, P. S., T. C. Chiu, M. T. Chen, K. Y. Wei, and Y. G. Chen, 2000: Planktic foraminifer fauna assemblage and sea surface temperature variations in a "Warm-Pool" South China Sea record of the past 400,000 years: Images Core MD972142. *J. Geol. Soc. China*, **43**, 467-496.